

Synthesis of N-doped Mesoporous Titania with High Visible-light Photocatalytic Activity

WANG Hui-Lei^{1,2}, LIU Xiao-Heng¹

(1. Key Laboratory for Soft Chemistry and Functional Materials, Nanjing University of Science and Technology, Ministry of Education, Nanjing 210094, China; 2. School of the Environment and Safety Engineering, Jiangsu University, Zhenjiang 212013, China)

Abstract: N-doped mesoporous titania was synthesized using polyethylene glycol (PEG) as template and Dimethyl Formamide (DMF) as nitrogen source. The physical and photophysical properties of the photocatalyst were characterized by X-ray diffraction (XRD), FTIR, BET, transmission electron microscope (TEM), UV-Vis diffuse reflectance spectra (DRS), and X-ray photoelectron spectra (XPS). PEG played an important role in the preparation process within mesoporous titania. The N-doped mesoporous titania possessed diameter of *ca.* 20 nm with anatase crystalline structure, and had absorption in the visible region. N-doped mesoporous titania samples showed excellent photocatalytic activity for methyl orange (MO) degradation under visible light irradiation, which could be attributed to synergistic effect between the retained alkoxyls and the nitrogen doping.

Key words: mesoporous titania; N- doping; photodegradation

Semiconductor TiO₂ is widely used because of its high photocatalytic activity, chemical stability, low cost and non-toxicity^[1]. However, the main drawback of TiO₂ is the need for UV radiation to excite electron-hole pairs because of its large band gap (3.2 eV for anatase). Many attempts have been made to make it active in the visible range, which include dye sensitization, metal ion doping and non-metal doping.

Non-metal doping is the most commonly used for decreasing the band gap. Extensive research work has been done on synthesis of N-doping, F-doping, and doping with carbon^[2-5]. Sato was the first to report on nitrogen doped titania^[6]. Nitrogen content that was more or less than the optimum content resulted in decreased photocatalytic activity.

Additionally, modification of semiconductors is another application of visible-light induced photocatalyst. Mesoporous materials with hierarchical and tunable pore architecture are getting considerable attention because of its potential applications in the field of catalysis, bio-medical engineering, energy storage and conversion, separation technology, *etc*^[7-12]. The preparation of mesoporous titania mainly relies on soft template (supra molecular assemblies of surfactants or block copolymers) and hard template (porous alumina, porous silica, porous carbon, polystyrene spheres)^[13-15].

As dispersion and soft template, polyethylene glycol (PEG) has been employed many times to prepare nanocrystalline TiO₂. Liu, *et al*^[16] reported an improved Sol-Gel method using PEG as a multifunctional agent for preparing ultrafine and crystallized TiO₂ powders without calcining step. With this background, it was attempted to synthesize mesoporous titania using PEG as soft template at 80°C.

In this work, we synthesized and characterized N-doped mesoporous titania photocatalysts with various levels of nitrogen doping, which used PEG as soft template. The new photocatalyst showed excellent photocatalytic activity for methyl orange oxidation under visible light irradiation ($\lambda \geq 400$ nm).

1 Materials and methods

The chemicals used for the synthesis were titanium (IV) tetrachloride, hydrochloric acid, polyethylene glycol 20000, n-butyl alcohol (AR, China) and Dimethyl Formamide (DMF).

1.1 Synthesis of N-doped TiO₂

All chemicals were analytical-grade reagents and were used without further purification. In a typical synthesis procedure, 5.7 g TiCl₄ was slowly added into 10 mL HCl under vigorous and constant stirring. Subsequently with

Received date: 2014-03-17; **Modified date:** 2014-06-10; **Published online:** 2014-06-20

Foundation item: National Natural Science Foundation of China(51272107); Natural Science Foundation of Jiangsu Province, China (BK2011024)

Biography: WANG Hui-Lei (1982–), female, PhD candidate. E-mail: wanghuilei1982@163.com

Corresponding author : LIU Xiao Heng, professor. E-mail: xhliu@mail.njust.edu.cn

300 mL *n*-butyl alcohol and 5 g PEG ($M = 20000$) added to the mixture under refluxing conditions at 80°C for 20 h, which was used to prepare mesoporous titania. A post-treatment to the above process, was carried out in DMF (0.5–15 mL) at 180°C for 24 h in a sealed Teflon container. The resulting product was obtained, thoroughly washed with distilled water, and finally dried in vacuum. The sample without a post-treatment was denoted a, others collected with 0.5, 2, 5, 10, 15 mL DMF were denoted b, c, d, e, f, respectively.

1.2 Characterization

The as-synthesized samples were characterized by X-ray diffraction (XRD) with a Bruker D8 diffractometer with monochromatic Cu $K\alpha$ radiation ($\lambda=0.1542$ nm). Transmission electron microscopy (TEM) observations were performed using a transmission electron microscopy (JEOL-2100) at 200 kV and a Gatan 794 charge-couple device (CCD) camera. The samples were ultrasonically dispersed in 5 mL deionized water for 5 min. Next, the solution was dropped to a copper grid. UV-visible spectra were recorded on a Shimadzu UV-2500 spectrophotometer in a 1 cm optical path quartz cuvette over a 200–800 nm range at room temperature. The chemical states of species in the TiO_2 samples were investigated using X-ray photoelectron spectra (XPS), employing Thermo ESCALAB 250 XPS with a monochromatic Al $K\alpha$ X-ray source system.

1.3 Photocatalytic measurement

The photocatalytic activities of the samples were evaluated by the photodegradation of MO in an aqueous solution at room temperature under visible light irradiation (VB). During the process, the catalyst (0.01 g) was suspended in a fresh dye aqueous solution ($C_0(\text{MO}) = 1 \times 10^{-5}$ mol/L, 50 mL). The suspension was ultrasonically dispersed for 10 min, then stirred in the dark for 30 min to allow an adsorption-desorption equilibrium of MO dye. After 30 min, the solution was illuminated whilst stirring. At a certain interval, a certain amount of sample (8 mL for the VB-induced reaction) was drawn from the system, centrifuged and then the absorption spectrum at 464 nm of the dye was monitored. The visible light irradiation source ($\lambda > 400$ nm) was obtained by putting an appropriate cut-off filter in the front of a 500 W Xe-lamp to completely remove wavelengths shorter than 400 nm. The photoreactor was placed a magnetic stirrer to ensure homogeneous mixing during irradiation.

2 Results and discussion

Figure 1 shows the SAXD patterns of sample a and sample e. Low angle peaks in the range of 2θ value 1° – 7° characteristics of ordered mesoporous structure were not

observed. It implies that the ordered mesoporous structure of samples a and e were all not formed^[17], and we can not calculate the pore diameter from Fig. 1.

XRD patterns of mesoporous titania and N-doped mesoporous titania are given in Fig. 2. Identification of titania phase, confirmed by comparison to accepted standard peaks from JCPDS. A series of characteristic peaks, corresponding to the (101), (004), (200), (105), (211) and (204) planes are observed, which can be indexed to anatase TiO_2 (JCPDS. 21-1272). It implies that crystal phase has no changes in the N-doping process.

FTIR spectra of mesoporous titania and N-doped mesoporous titania are shown in Fig. 3. The peaks corresponding to N–H₂ stretching (3690 cm^{-1}) and N–H bending (1573 cm^{-1}) indicate the presence of nitrogen in the synthesized photocatalyst. Figure 3b–3f show the FTIR spectra of N-doped mesoporous titania with different volume of DMF respectively. Compared with the spectra in Fig. 3a, the peak at 1618 cm^{-1} was retained in all the photocatalyst. Peak at 1573 cm^{-1} (N–H bending vibrations) of bare DMF was retained in samples e and f, but got eliminated in case of samples b, c and d. Peak at 1573 cm^{-1} were present in photocatalysts e and f, but the peak intensity of sample f was much lower. FTIR study interprets that N–H bending vibrations peaks are prominent and shows the presence of nitrogen in the photocatalyst. However,

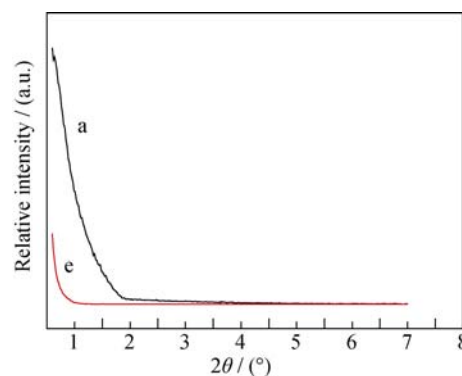


Fig. 1 SAXD patterns of sample a and sample e

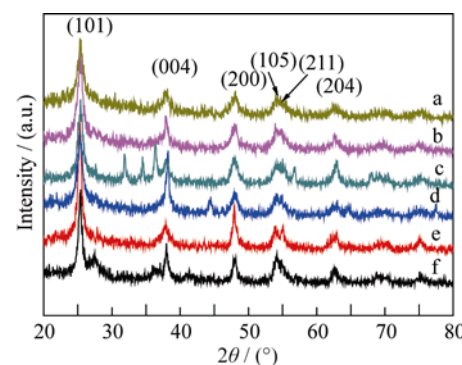


Fig. 2 XRD patterns of (a) mesoporous titania and (b-f) N-doped mesoporous titania with different volume of DMF

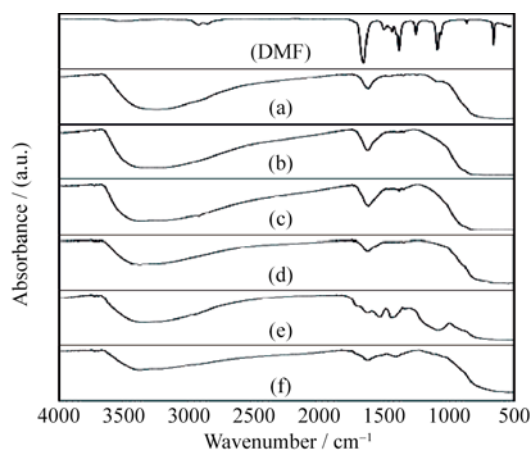


Fig. 3 FTIR spectra of (a) mesoporous titania and (b-f) N-doped mesoporous titania with different volume of DMF (DMF Dimethyl Formamide)

DMF might be just chelated to the surface of the TiO_2 instead of doping, so we need to XPS analysis further to confirm the atom level doping.

XPS survey spectrum and N_{1s} core level of the sample e were measured (Fig. 4). It contains not only Ti, O and C, with sharp photoelectron peaks appearing at binding energies of 458 eV ($\text{Ti}2p$), 529 eV ($\text{O}1s$) and 285 eV ($\text{C}1s$), but also a small amount of N atom (binding energies at 401 eV). It shows the high resolution XPS spectra of N_{1s} . Three XPS peaks at 400, 401 and 404 eV were observed. Different N_{1s} peak positions represent various forms of N-doped titania. Most N species in the sample e exist in form of nitrides such as N in the O–Ti–N and Ti–O–N linkage, corresponding to the (BE) of 400 eV and 401 eV. Sato observed a peak at 400 eV for TiO_2 power heated in the presence of ammonium chloride^[18]. In later studies, the peak at about 399.7 eV was frequently observed for N-doped TiO_2 materials^[19]. Therefore, it was believed that at least two kinds of nitrogen doping were responsible for the visible light photoactivity.

Figure 5 shows the nitrogen adsorption-desorption

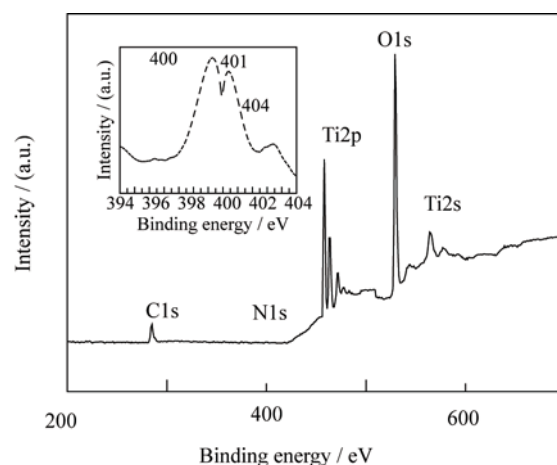


Fig. 4 XPS survey spectrum and N_{1s} core level of the sample e

isotherms and pore size distribution curve of the sample a and sample e. All the adsorption isotherm of sample a and sample e can be classified as type IV (BDDT classification), with a H_2 hysteresis, which appear to the mesoporous structure was open ends with cylindrical type, and Aperture size of the sample was uniformity. It can be found that, comparing sample e with sample a, BET surface areas increase obviously ($S_{\text{BET}}[\text{a}]=176.64 \text{ m}^2/\text{g}$ $S_{\text{BET}}[\text{e}]=225.39 \text{ m}^2/\text{g}$). It is possible that the nanoparticles of the sample e was more tiny, which agrees well with the TEM images shown in Fig. 6.

Figure 6 shows the TEM images of representative samples. Figure 6(A) is a low-magnification cross-sectional TEM image of sample a, revealing that the mesoporous titania is formed by aggregated clusters consisting of nanoparticles, and this is how to form disorder mesoporous structure, which agrees with the SAXD patterns as shown in Fig. 1. The high-magnification of the individual spheres (Fig. 6(B)) shows a highly rough surface with mesoporous structure. The formation of mesoporous structure is due to the PEG as a soft template and the agglomeration of nanoparticles. After post-process method, the sample e (Fig. 6(C), 6(D) and 6(E)) is more tiny than the sample

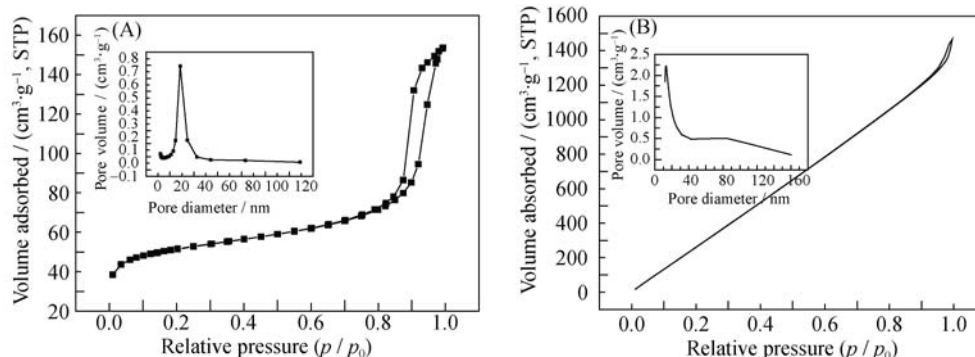


Fig. 5 (A) N_2 adsorption-desorption isotherms and pore size distributions (inset) of sample a; (B) N_2 adsorption-desorption isotherms and pore size distributions (inset) of sample e

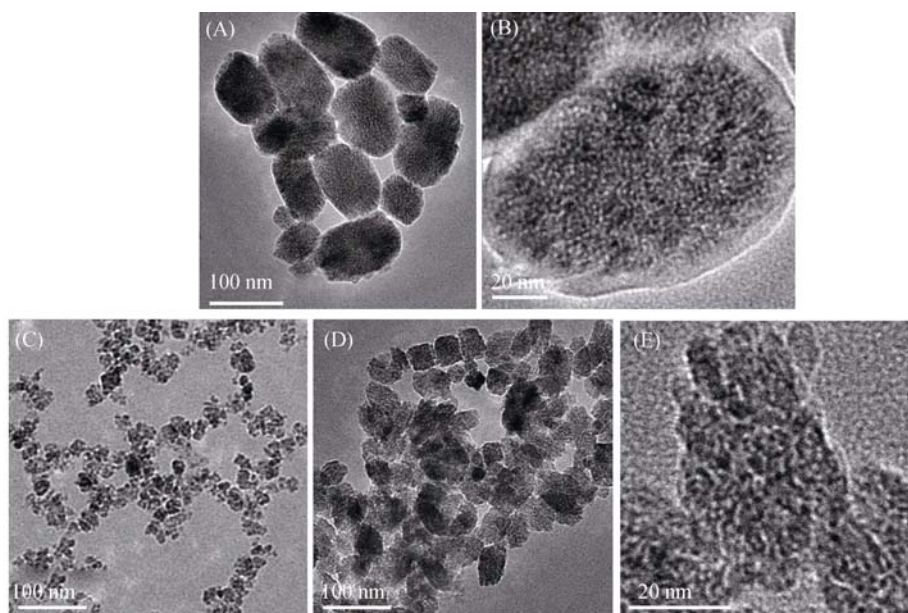


Fig. 6 TEM images of mesoporous titania (sample a) (A, B) and N-doped mesoporous titania (sample e) (C, D, E)

a, which results in larger specific surface areas and increasing in photocatalytic activity. The sample e possesses diameter of *ca.* 20 nm with anatase crystalline structure. It may be mesoporous titania interact with DMF which results in the broken particles under high temperature and high pressure.

UV-Vis diffused reflectance spectra of mesoporous titania and N-doped mesoporous titania along with Degussa P25 are given in Fig. 7. The wavelength maxima observed for all the samples are showed in Table 1. λ_{\max} values indicating that the wavelength response range is in visible region. N-doped mesoporous titania shows remarkable red shift as compared to P25 photocatalyst^[20].

Band gap energy has been calculated for all photocatalysts by using the formula:

$$E_g = 1240/\lambda_g \text{ (eV)}$$

Where λ_g is the wavelength value obtained from UV-DRS spectra.

These results confirm lowering of band gap energy due to N-doping in mesoporous titania by using the present method^[21].

The possible nitridation process: Firstly, DMF can hydrolyze to produce $\text{NH}(\text{CH}_3)_2$ and HCOOH in the presence of water during the hydrothermal process. Secondly, $\text{NH}(\text{CH}_3)_2$ can continually adsorb on the surface of TiO_2 . Thirdly, the nitridation occurs by replacing the oxygen atom in the TiO_2 with the nitrogen atom in the DMF, resulting in the formation of the O-Ti-N and the Ti-O-N species. A similar mechanism has been reported^[22-23]. To explore the photocatalytic activity of the prepared samples in the visible range, degradation of MO by visible light was investigated. The photocatalytic behaviour of P25 was also measured as control. The photocatalytic activity of various types of photocatalysts was represented by the

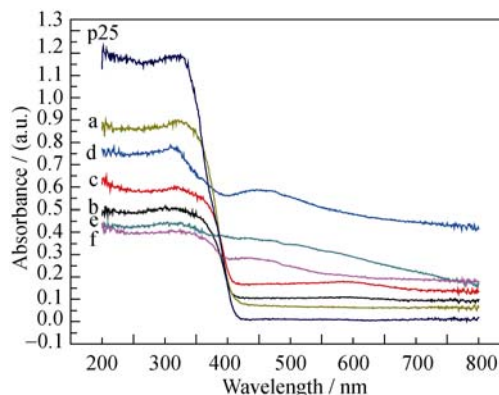


Fig. 7 UV-DRS spectra of mesoporous titania (a) and N-doped mesoporous titania with different volume of DMF and P25 (b-f)

Table 1 Wavelength value obtained from UV-DRS spectra and band gap energy values obtained for the synthesized photocatalysts

Catalyst	λ_g	Band gap energy/eV
P25	387	3.20
a	394	3.14
b	408	3.04
c	410	3.02
d	450	2.76
e	506	2.45
f	475	2.61

ratio of removed concentration to initial concentration of $\text{MO}[(C_0 - C)/C_0]$, as a function of irradiation time. As illustrated in Fig. 8, MO degradation with P25 was negligible (about less than 3%), and mesoporous titania could degrade nearly 10% of MO result in its highly rough surface. N-doped mesoporous titania with various levels of nitrogen doping could degrade 70% to 95% of MO in 120 min under visible-light irradiation, respectively.

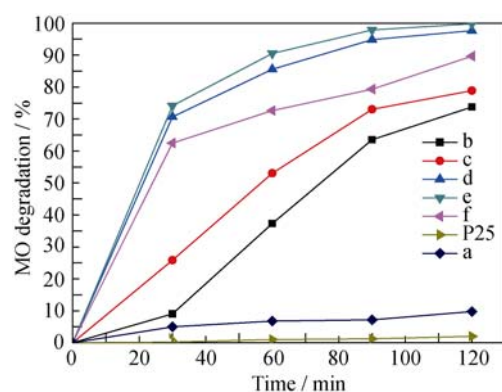


Fig. 8 Photocatalytic degradation of MO under visible light irradiation

Mesoporous titania (a) and N-doped mesoporous titania with different volume of DMF (b-f)

3 Conclusions

Mesoporous titania photocatalysts with various levels of nitrogen doping are prepared by a convenient and effective method. These photocatalysts exhibit higher visible-light photoactivity in liquid-phase MO degradation than that of Degussa P25, which can be assigned to synergistic effect between the retained alkoxy groups and the nitrogen doping.

References:

- [1] CHEN X, MAO S S. Titanium dioxide nanomaterials: synthesis, properties, modifications, and applications. *Chem. Rev.*, 2007, **107**(7): 2891–2959.
- [2] IRIE H, WATANABE Y, HASHIMOTO K. Nitrogen-concentration dependence on photocatalytic activity of $\text{TiO}_{2-x}\text{N}_x$ powders. *J. Phys. Chem. B*, 2003, **107**(23): 5483–5486.
- [3] XU T H, SONG C L, LIU Y, *et al.* Band structures of TiO_2 doped with N, C and B. *J. Zhejiang Univ. Sci. B*, 2006, **7**(4): 299–303.
- [4] LI D, HANEDA H, LABHSETWAR N K, *et al.* Visible-light-driven photocatalysis on fluorine-doped TiO_2 powders by the creation of surface oxygen vacancies. *Chem. Phys. Lett.*, 2005, **401**(4/5/6): 579–584.
- [5] LI D, HANEDA H, HISHITA S, *et al.* Fluorine-doped TiO_2 powders prepared by spray pyrolysis and their improved photocatalytic activity for decomposition of gas-phase acetaldehyde. *J. Fluorine Chem.*, 2005, **126**(1): 69–77.
- [6] SATO S. Photocatalytic activity of NO_x -doped TiO_2 in the visible light region. *Chem. Phys. Lett.*, 1986, **123**(1/2): 126–128.
- [7] KRESGE C T, LEONOWICZ M E, ROTH W J, *et al.* Ordered mesoporous molecular sieves synthesized by a liquid-crystal template mechanism. *Nature*, 1992, **359**: 710–712.
- [8] DAVIS M E. Ordered porous materials for emerging applications. *Nature*, 2002, **417**: 813–821.
- [9] YANG P, ZHAO D, MARGOLESE D I, *et al.* Generalized syntheses of large-pore mesoporous metal oxides with semicrystalline frameworks. *Nature*, 1998, **396**: 152–155.
- [10] BACH U, LUPO D, COMTE P, *et al.* Solid-state dye-sensitized mesoporous TiO_2 solar cells with high photon-to-electron conversion efficiencies. *Nature*, 1998, **395**: 583–585.
- [11] HUO Q, LEON R, PETROFF P M, *et al.* Mesostructure design with gemini surfactants: supercage formation in a three-dimensional hexagonal array. *Science*, 1995, **268**(5215): 1324–1327.
- [12] SOLER-ILLIA G J, SANCHEZ C, LEBEAU B, *et al.* Chemical strategies to design textured materials: from microporous and mesoporous oxides to nanonetworks and hierarchical structures. *Chem. Rev.*, 2002, **102**(11): 4093–4138.
- [13] SHIBATA H, OGURA T, MUKAI T, *et al.* Direct synthesis of mesoporous titania particles having a crystalline wall. *J. Am. Chem. Soc.*, 2005, **127**(47): 16396–16397.
- [14] WU C, OHSUNA T, KUWABARA M, *et al.* Formation of highly ordered mesoporous titania films consisting of crystalline nanopillars with inverse mesospace by structural transformation. *J. Am. Chem. Soc.*, 2006, **128**(14): 4544–4545.
- [15] CHAE W, LEE S, KIM Y. Templating route to mesoporous nanocrystalline titania nanofibers. *Chem. Mater.*, 2005, **17**(12): 3072–3074.
- [16] LIU H X, YANG J, WANG L, *et al.* An improvement on Sol-Gel method for preparing ultrafine and crystallized titania powder. *Materials Science and Engineering A*, 2000, **289**: 241–245.
- [17] FEI H, LUI Y, LI Y, *et al.* Selective synthesis of borated mesoporous and mesoporous spherical TiO_2 with high photocatalytic activity. *Micropor. Mesopor. Mater.*, 2007, **102**(1/2/3): 318–324.
- [18] SATO S. Photocatalytic activity of NO_x -doped TiO_2 in the visible light region. *Chem. Phys. Lett.*, 1986, **123**(1/2/3): 126–128.
- [19] LIU G, ZHAO Y N, SUN C H, *et al.* Synergistic effects of B/N doping on the visible-light photocatalytic activity of mesoporous TiO_2 . *Angew. Chem. Int. Ed.*, 2008, **47**(24): 4516–4520.
- [20] XU J, LI J, DAI W, *et al.* Simple fabrication of twist-like helix N,S-codoped titania photocatalyst with visible-light response. *Appl. Catal. B: Environ.*, 2008, **79**(1): 72–80.
- [21] KOROSI L, DEKANY I. Preparation and investigation of structural and photocatalytic properties of phosphate modified titanium dioxide. *Colloids Surf. A*, 2006, **280**(1/2/3): 146–154.
- [22] LI L, LIU C Y. Facile Synthesis of anatase–brookite mixed-phase N-doped TiO_2 nanoparticles with high visible-light photocatalytic activity. *Eur. J. Inorg. Chem.*, 2009, **2009**(20): 3727–3733.
- [23] LI H X, LI J X, HUO Y N. Highly active TiO_2N photocatalysts prepared by treating TiO_2 precursors in NH_3 /ethanol fluid under supercritical conditions. *J. Phys. Chem. B*, 2006, **110**(4): 1559–1565.

高活性氮掺杂介孔二氧化钛的合成及性能研究

王慧蕾^{1,2}, 刘孝恒¹

(1. 南京理工大学 化工学院, 软化学与功能材料教育部重点实验室, 南京 210094; 2. 江苏大学 环境与安全工程学院, 镇江 212013)

摘 要: 采用水热法, 以聚乙二醇(PEG)为模板, N,N-二甲基甲酰胺为氮源, 制备了氮掺杂的介孔二氧化钛。并用 X 射线粉末衍射(XRD)、傅立叶红外光谱(FTIR)、BET、透射电子显微镜(TEM)、紫外-可见漫反射谱(DRS)和 X 射线光电子能谱(XPS)等技术手段对制备样品进行了表征。结果表明: 所合成的样品具有锐钛矿结构, 直径约 20 nm, 并且具有一定的可见光活性。以甲基橙(MO)为光降解模型, 样品在可见光区表现出了较好的催化活性, 这取决于烷氧基和氮掺杂的协同效应。

关 键 词: 介孔二氧化钛; 氮掺杂; 光催化

中图分类号: TQ174

文献标识码: A